Astronomy & Astrophysics manuscript no. 15347
February 10, 2011

© ESO 2011

arXiv:1012.5831v2 [astro-ph.CO] 9 Feb 2011

Fossil groups in the Millennium simulation

Their environment and its evolution

Eugenia Díaz-Giménez[1], Ariel Zandivarez[1], Robert Proctor[2], Claudia Mendes de Oliveira[2] and L. Raul Abramo[3]

[1] IATE (CONICET-UNC) & OAC (UNC). Laprida 854, Córdoba 5000. Argentina
e-mail: `eugeniadiazz@gmail.com, arielz@mail.oac.uncor.edu`
[2] IAG, USP. Rua do Matão 1226, São Paulo. Brazil
e-mail: `rproctor@astro.iag.usp.br, oliveira@astro.iag.usp.br`
[3] Instituto de Física, Universidade de São Paulo. CP 66318, CEP 051314-970, São Paulo. Brazil.
e-mail: `abramo@fma.if.usp.br`

Received Month XX, year; accepted XX XX, year

ABSTRACT

Context. Fossil systems are defined to be X-ray bright galaxy groups (or clusters) with a two-magnitude difference between their two brightest galaxies within half the projected virial radius, and represent an interesting extreme of the population of galaxy agglomerations. However, the physical conditions and processes leading to their formation are still poorly constrained.
Aims. We compare the outskirts of fossil systems with that of normal groups to understand whether environmental conditions play a significant role in their formation. We study the groups of galaxies in both, numerical simulations and observations.
Methods. We use a variety of statistical tools including the spatial cross-correlation function and the local density parameter Δ_5 to probe differences in the density and structure of the environments of 'normal' and 'fossil' systems in the Millennium simulation.
Results. We find that the number density of galaxies surrounding fossil systems evolves from greater than that observed around normal systems at z=0.69, to lower than the normal systems by z=0. Both fossil and normal systems exhibit an increment in their otherwise radially declining local density measure (Δ_5) at distances of order 2.5 r_{vir} from the system centre. We show that this increment is more noticeable for fossil systems than normal systems and demonstrate that this difference is linked to the earlier formation epoch of fossil groups. Despite the importance of the assembly time, we show that the environment is different for fossil and non-fossil systems with similar masses and formation times along their evolution. We also confirm that the physical characteristics identified in the Millennium simulation can also be detected in SDSS observations.
Conclusions. Our results confirm the commonly held belief that fossil systems assembled earlier than normal systems but also show that the surroundings of fossil groups could be responsible for the formation of their large magnitude gap.

Key words. Methods:statistical– Galaxies:clusters:general– Galaxies:evolution

1. Introduction

The hierarchical structure formation paradigm is successful in predicting many of the properties of galaxy groups and clusters. However, to-date, the specific conditions and processes that lead to the formation of a 'fossil' system have still to be unequivocally identified.

'Fossil' systems are defined as spatially extended X-ray sources with an X-ray luminosity $L_X > 10^{42}\ h_{50}^{-2}\ erg\ s^{-1}$ whose optical counterpart is a bound system of galaxies with $\Delta M_{12} > 2$ mag, where ΔM_{12} is the difference in absolute magnitude in R-band between the brightest and the second brightest galaxies located within half the projected virial radius of the systems. (r_{vir}) (Jones et al. 2003). Broadly speaking, this means that fossil systems consist of a relatively isolated, luminous, early-type galaxy embedded in a swarm of much smaller galaxies and an extended X-ray halo. These systems may therefore be of considerable importance as the place of formation of giant elliptical galaxies.

The question then naturally arises: how do these systems form? One suggested scenario is that fossil systems form when a group or cluster remains undisturbed for a significant fraction of a Hubble time. Within the context of hierarchical structure formation, this means that fossil systems would have assembled their dark matter halos earlier than normal groups, thus leaving enough time for $L^\star$ objects to merge into the central galaxy by dynamical friction. In other words, any large, centrally located satellite galaxies would have been tidally stripped, disrupted, and finally cannibalised by the brightest galaxy, naturally producing the characteristic magnitude gap ($\geq 2mag$). In the present epoch, the central regions of fossil systems would therefore exhibit the observed lack of $L^\star$ galaxies, but the fainter end of the luminosity function would remain intact, because of the longer timescale of dynamical friction for low mass galaxies.

The next question to arise is then: which systems are most likely to experience this kind of evolution? Much effort has been devoted to answering this question. Beside minor differences in the definition of fossil groups, the fossil group phenomenon has been studied from the broad range of observational, analytical, numerical, and semi-analytical points of view (Vikhlinin et al. 1999; Jones et al. 2003; D'Onghia et al. 2005; Mendes de Oliveira et al. 2006; Cypriano et al. 2006; Khosroshahi et al. 2006; Milosavljević et al. 2006; van den Bosch et al. 2007; Sales et al. 2007; von Benda-Beckmann et al. 2008; Mendes de Oliveira & et al. 2008). Most of these works have been motivated by the questions of whether the large magnitude difference in fossil groups implies that they are a distinct class of objects or they simply represent a tail of the cluster distribution.

Since the number of fossil systems identified observationally is rather low, N-body cosmological simulations are of considerable importance, as they allow us to perform statistical analysis. The largest cosmological numerical simulation presently available is the ”Millennium simulation” (Springel et al. 2005, hereafter MS). When combined with semi-analytical models of galaxy formation, this simulation constitutes a useful tool in addressing open issues surrounding the formation of fossil systems. Three important studies used this tool to analyse the evolution of fossil groups. On the one hand, Dariush et al. (2007) concluded that fossil systems identified in the MS assembled a larger fraction of their masses at higher redshifts than non-fossil groups. Therefore, they suggest that the most likely scenario for fossil groups is that they are not a distinct class of object but simply examples of groups/clusters that collapsed early. Dariush et al. (2010) then suggested refinements to the fossil definition to enhance its efficiency in detecting old systems. On the other hand, Díaz-Giménez et al. (2008) studied the first ranked galaxies in the MS, comparing the merger history of the central galaxies in fossil and normal systems. By analysing central galaxies with equal stellar mass distributions, they found that, despite the earlier assembly time of fossil systems, first ranked galaxies in fossil groups assembled half of their final mass and experienced their last major merger *later* than their non-fossil counterparts, which implies that they followed a different evolutionary pathway. Consensus has clearly yet to be reached regarding the nature of fossil systems.

Few works have studied the environment of fossil systems or the influence that it could have had on their formation, mainly because there are too few known fossil groups to allow a reliable statistical analysis. However, observationally, it has been suggested that fossil systems inhabit under-dense regions (Jones et al. 2003). On the other hand, von Benda-Beckmann et al. (2008) used numerical simulations to conclude that there is no tendency for fossil systems to be preferentially located in low density environments. They also showed that many galaxy groups and clusters may undergo a fossil phase in their lives, but may not necessarily still be fossil systems at $z = 0$ because of the infall of $L^{\star}$ galaxies from the large-scale environment. However, we note that their study was limited to groups of relatively low virial masses ($1 - 5 \times 10^{13}\ h^{-1}\ \mathcal{M}_{\odot}$), which might not encompass the characteristic X-ray emission of observationally selected fossil systems (Dariush et al. 2007). In addition, several works on galaxy groups have shown that their virial masses and the assembly times strongly depend on their environment (Gao et al. 2005; Berlind et al. 2006; Wetzel et al. 2007; Jing et al. 2007).

In this work, we attempt to obtain a clearer picture of fossil systems and their environments by analysing the surroundings of systems extracted from the MS. Throughout, we refer to groups and clusters that meet the ’fossil’ criteria above as ’fossil systems’ or simply ’fossils’ and those that do not meet the criteria as ’non-fossils’ or ’normal’ systems.

The layout of this paper is as follows: In Sect. 2, we describe the construction of the sample of fossil and non-fossil groups. In Sect. 3, we study the outskirts of these groups using the two-point cross-correlation function, while in Sect. 4, we describe their environment by means of the local density profile. The analysis of the differences between the environments of fossils and non-fossils are carried out in Sect. 5. A comparison with observationally selected fossil groups is performed in Sect. 6, while we summarise our conclusions in Sect. 7.

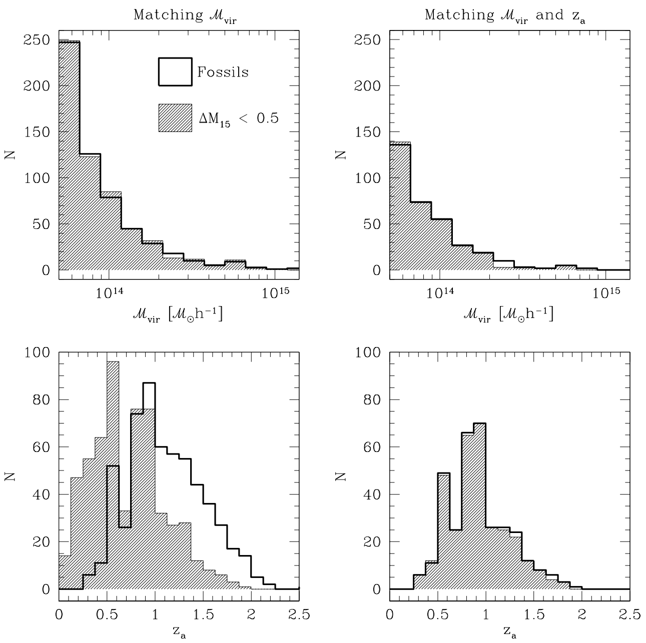

Fig. 1. *Upper panels* show the virial mass distributions of the samples of fossil (*empty*) and $\Delta M_{12} < 0.5mag$ (*filled*) groups in the MS, while *lower panels* show the assembly time distributions. *Left panels*: “Mass-matched” samples. Non-fossils that were selected to reproduce the same virial mass distribution of fossil groups in order to avoid a mass bias. *Right panels*: “Assembly-matched” samples. Fossils and non-fossils were selected to have both similar virial mass *and* assembly time distributions.

2. The samples

Our samples of fossil and normal groups were extracted from the Millennium Simulation (Springel et al. 2005) combined with a semi-analytic model of galaxy formation. These samples were defined in Díaz-Giménez et al. (2008). Here, we briefly summarise their main characteristics:

- The MS evolved 10 billion (2160^3) dark matter particles within a periodic box of 500 $h^{-1}\ Mpc$ in a Lambda cold dark matter (ΛCDM) cosmology with parameters: $\Omega_m = 0.25$, $\Omega_{\Lambda} = 0.75$, $\sigma_8 = 0.9$, and $h = 0.73$.
- To extract galaxies from the MS, we adopted the run of De Lucia & Blaizot (2007)’s semi-analytic model, which provides positions, velocities, absolute magnitudes (BVRIK), etc. The final output at $z = 0$ contained $\sim 10^7$ galaxies with absolute magnitudes $M_R - 5 log\, h < -17.4$ and stellar masses higher than $3 \times 10^8\ h^{-1}\ \mathcal{M}_{\odot}$.
- Groups were identified at the z=0 output of the simulation using a friends-of-friends algorithm in real space with a linking length of 0.2 of the mean particle density and cross-correlated with the DM halos identified in the MS (Díaz-Giménez et al. (2008)). Their merging history was followed back in time to study the evolutionary behaviour of galaxies inside and outside the virial radii of the systems. Virial radii and positions of the groups at the different outputs used throughout this work were extracted from the publicly available information of the MS+semi-analytic model[1].

---

[1] The Millennium simulation, performed by the Virgo Consortium, is available at http://www.mpa-garching.mpg.de/millennium

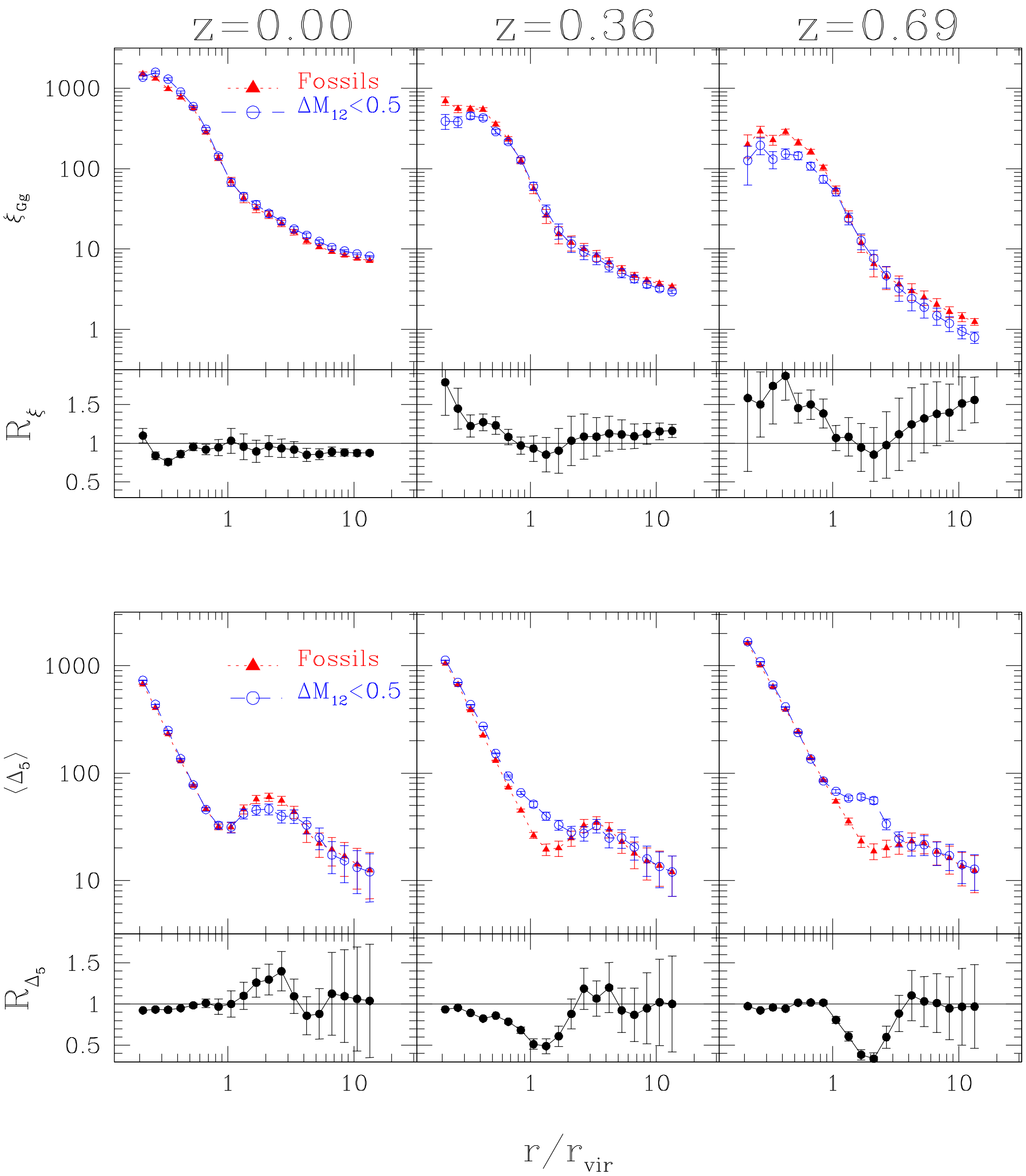

Fig. 2. *Top panels*: Group-galaxy cross-correlation functions of the mass-matched samples (ξ_{G-gal}). *Upper panels*: ξ_{G-gal} in the MS as a function of the normalised group-centric distance. *Filled triangles* (*dotted lines*) correspond to fossil groups, while *open circles* (*dashed lines*) correspond to normal groups with a magnitude gap ΔM_{12} smaller than 0.5*mag*. Error bars are computed using an analytic formula for the Poisson error in the clustering signal (Peacock 1999). *Lower panels*: Ratios of cross-correlation functions (R_ξ) for fossils and groups with $\Delta M_{12} < 0.5$*mag*. Error bars are computed using the usual formula of error propagation. *Panels from left to right*: Different stages of the group evolution (see upper labels). *Bottom panels:* Local over-density profile of galaxies around groups (Δ_5). *Upper panels*: Δ_5 in the MS as a function of the normalised group-centric distance. *Filled triangles* (*dotted lines*) correspond to galaxies around fossils groups, while *open circles* (*dashed lines*) correspond to galaxies around normal groups with $\Delta M_{12} < 0.5$ *mag*. Error bars represent the 35th and the 65th percentiles in the local density distribution at each distance bin. *Lower panels*: Ratios of local density profiles (R_{Δ_5}) of fossils and groups with $\Delta M_{12} < 0.5$*mag*. Error bars are computed using the usual formula of error propagation. *Panels from left to right* correspond to the stages of the group evolution (see upper labels).

Specifically, virial radii were estimated using the virial theorem, with the virial masses and velocity dispersions obtained from the MS database. The virial masses used for these estimates were the masses within the radius where the halo has an over-density corresponding to the value at virialisation in the top-hat collapse model for the ΛCDM cosmology.

- Fossil systems were selected from the sample of systems identified at $z = 0$ to have virial masses higher than $5 \times 10^{13}\, h^{-1}\, \mathcal{M}_\odot$ and absolute magnitude difference between the first and second brightest galaxies (ΔM_{12}) greater than 2 (in the R-band) when considering objects within 0.5 r_{vir}. This lower cut-off in virial masses maximises the probability that the selected systems are X-ray emitters (Dariush et al. 2007). The final sample comprises 591 fossils. We note that there is a small difference between this sample and the one obtained by Díaz-Giménez et al. (2008). This is due to the lack

of some physical properties of some systems in particular redshift snapshots used in our analysis. The virial mass distribution of fossil systems can be seen in the *upper left panel* of Fig. 1 (*empty histogram*).
- Following the procedure of Díaz-Giménez et al. (2008), we define a sample of non-fossils in order to directly compare with the fossil sample. The non-fossil sample comprises groups with the same lower limit in virial mass, but having $\Delta M_{12} < 0.5 mag$. This sample of non-fossils comprises 1997 systems. It is well-known that cluster formation histories depend strongly on the mass of the systems. Consequently, differences in the virial mass distributions of the fossil and non-fossil samples could introduce bias into the results. Therefore, we extracted a sub-sample of 591 non-fossil groups with the same virial mass distribution (Kolmogorov-Smirnov coefficient > 0.98) as the sample of fossils (the "mass-matched" samples; see *upper left panel* of Fig. 1). The *lower left panel* of Fig. 1 shows the assembly time distributions (time at which groups have assembled half of their final virial mass) for the samples of fossil and non-fossil ($\Delta M_{12} < 0.5$ *mag*) groups.
- To test the effects of assembly time on our statistics, we also defined samples of fossils and non-fossils with matched assembly times (right panels, Fig 1). We refer to these as the "assembly-matched" samples (although we note that the samples are both assembly-time- *and* mass-matched).
- We also studied the remaining sample of normal groups with $0.5 \leq \Delta M_{12} \leq 2$, which comprises 6881 groups. We divided this sample of normal systems into 15 sub-samples, each of them resembling the fossil sample in terms of the number of systems and virial mass distributions.

We note that we are unable to easily assess the effects of using a semi-analytic model other than the De Lucia & Blaizot (2007) model used in this work. However, given that all similar models that reproduce the galaxy luminosity function reasonably well, we would expect any effects to be small. We particularly note that the De Lucia & Blaizot model is one of the best at reproducing the bright end of the luminosity function (Bertone et al. 2007), which is of particular importance when measuring the ΔM_{12} parameter that defines fossil groups.

We note that our fossil sample is comprised of groups that exhibit $\Delta M_{12} > 2$ at z=0, and does not include groups that had $\Delta M_{12} > 2$ at higher redshift, but became 'normal' again by z=0 (as suggested by von Benda-Beckmann et al. 2008). The presence of these groups in our normal group samples can only serve to reduce any differences between our fossil and non-fossil samples and therefore does not affect our *qualitative* analysis.

3. The group-galaxy cross-correlation function

The spatial group-galaxy cross correlation function, $\xi_{Gg}(R)$, is defined such that the probability dP of finding a galaxy in volume element dV at distance R from the centre of a group is

$$dP = \bar{\eta}\,[1 + \xi_{Gg}(R)]dV,$$

where $\bar{\eta}$ is the mean number density of galaxies in the whole MS. The quantity $\xi_{Gg}(R)$ is therefore equivalent to the radially averaged number over-density profile. To increase the statistical significance of our results, we averaged the values for all groups after scaling to take into account the different group sizes. This is achieved by normalising the group-centric distances to the virial radius of each group ($R = r/r_{\rm vir}$). We refer to everything that lies farther than one virial radius from the group centre as the "environment" of the system.

At each stage in our analysis, a comparison was made between normal groups having $0.5mag < \Delta M_{12} < 2mag$ and those with $\Delta M_{12} < 0.5mag$. We found no differences between these two samples of normal groups at any stage. Therefore, throughout this paper we present the comparison of our fossil sample with the $\Delta M_{12} < 0.5mag$ sample.

To follow the evolution of the environment around groups, we chose three different redshift snapshots in the MS: z= 0.00, 0.36, and 0.69. The highest redshift value (0.69) represents the time by which 90% of fossil groups have assembled half of their final virial mass, while the middle redshift value (0.36) represents the time by which 90% of non-fossil groups have assembled half of their final virial mass. These characteristic times are inferred from the assembly time distributions shown in the lower left panel of Fig. 1.

The top panels of Fig. 2 show the cross-correlation functions obtained for the mass-matched samples of fossil and non-fossil ($\Delta M_{12} < 0.5mag$) groups, where the evolution of these functions is shown by the three redshift snapshots. We explored the cross-correlation functions out to a normalised distance of $\sim 10\ r_{vir}$ which represents a median distance of $\sim$ 17 h^{-1}Mpc (see. Sect. 4). Since the mean-intergroup separation for systems with virial masses higher than $5 \times 10^{13}\ h^{-1}\ \mathcal{M}_{\odot}$ is approximately 20 h^{-1}Mpc (Zandivarez et al. 2003), this limit in normalised clustercentric distances minimises the risk of the spatial superimposition of groups in our main samples. At all stages, all these cross-correlation functions show a clear transition from the 'one-halo' to the 'two-halo' regimes at the virial radius of the groups (Yang et al. 2005). In general, the one-halo term dominates the total contribution in the non-linear regime, while the two-halo term captures the large-scale correlations in the linear regime.

Starting at $z = 0.69$ (Fig. 2; upper right panel), the number density within the groups ($< 1\ r_{vir}$) is higher for fossils than non-fossils. At this redshift, this may be because most fossil groups unlike normal groups, have already assembled half of their final masses. Beyond 3 r_{vir}, the environments of fossils exhibit higher densities than normal groups. This is consistent with the earlier formation time of fossil groups, since halos forming in higher density environments collapse earlier (Sheth & Tormen 2004; Harker et al. 2006). There is a transition region between 1 r_{vir} and 3 r_{vir} where the environments around fossils and non-fossils looks similar (in terms of number density).

By z=0.36, both fossil and non-fossil systems have clearly evolved. The evolution both inside and outside of the virial radius is such that fossil and non-fossil systems have become more similar. Within the virial radius, this is to be expected since, by this time, most normal groups have also assembled more than 50% of their final mass.

At z=0, the ratio $R_{\xi} = \xi_{Fg}/\xi_{Ng}$ indicates that fossils appear to have slightly fewer galaxies within half a virial radius than normal groups. This may simply reflect that the central galaxies of fossils have cannibalised their neighbours to produce the two magnitude gap. There is again a 'transient' region between 0.5 r_{vir} and 2.5 r_{vir} where the global densities around both classes look very similar. Beyond this region, the environment of fossil systems at redshift zero has a slightly *lower* density than around normal systems.

A possible cause of the local density differences at high redshift is revealed in the *lower panel* of Fig. 3, which shows the evolution of the halo masses with redshift. Although both fossil and non-fossil samples reach the same final masses (by construction), at earlier times fossil groups can be seen to have higher

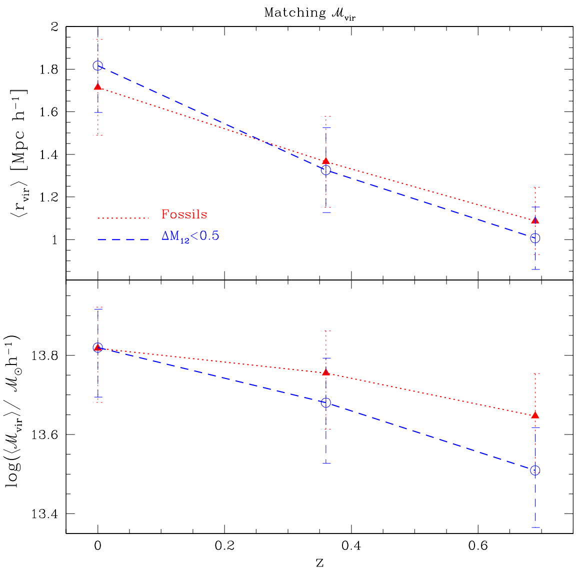

Fig. 3. Median values of virial radii (*upper panel*) and masses (*lower panel*) as a function of redshift for fossils (*dotted line*) and $\Delta M_{12} < 0.5 mag$ groups (*dashed line*). Error bars are the 25th and 75th percentiles.

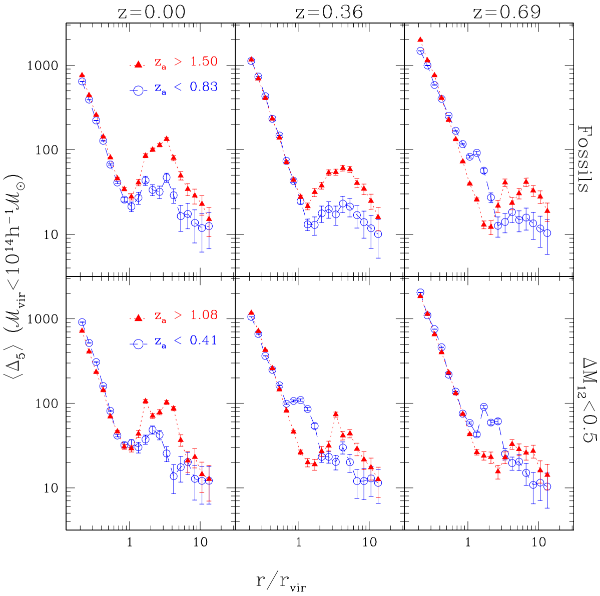

Fig. 4. Local over-density profile of galaxies around fossil (*upper panel*) and non-fossil (*lower panel*) groups in the MS as a function of the normalised group-centric distance. *Filled triangles* correspond to the sub-sample of systems with early assembly times, while *open circles* correspond to a sub-sample with later assembly times. Error bars are the 35th and the 65th percentiles of the local density distribution at each distance bin.

masses. This figure therefore suggests that the mass growth rate of fossils differs from that of non-fossils. However, these differences in halo mass evolution could be a consequence of different assembly times, since halos forming earlier are thought to form in higher density regions and also to have had more time to gain mass. This point will be addressed in Sect. 5, where we discuss the mass- *and* assembly-time matched samples.

4. The local density profile

To continue our analysis of the environment around galaxy systems, we also study the local over-density profile $\langle \Delta(r/r_{vir}) \rangle$. This statistic measures the local density around each galaxy and therefore contains information about the local clustering (clumpiness) of the groups.

The local density, η_N, is measured for every galaxy in and around groups. It is computed as the number density within a sphere of radius defined by the distance (d) to its N-*th* nearest neighbour, i.e.

$$\eta_N = \frac{3N}{4\pi d_N^3}.$$

The local over-density is then given by

$$\Delta_N = \frac{\eta_N - \overline{\eta}_N}{\overline{\eta}_N},$$

where $\overline{\eta}_N$ is the mean local density in the simulation. The local over-density profile is obtained by computing the median values of the over-density associated with each galaxy as a function of the 3D-normalised cluster-centric distance, i.e., $\langle \Delta_N(r/r_{vir}) \rangle$. The N value was tested using two different values of 5 and 10, and very similar results were obtained. We therefore show all our results using $N = 5$. As in the previous section, no significant differences were found between the results for normal groups having $0.5\ mag < \Delta M_{12} < 2\ mag$ and those with $\Delta M_{12} < 0.5\ mag$.

The local over-density profile is shown in the bottom panels of Fig. 2. It can be seen that, as expected, the local over-density of galaxies diminishes as we approach and pass through the virial radius. However, there is an increase in the local over-density around 2-4 r_{vir} (the "bump")[2]. This suggests that either there is a sudden increase in the global density at this radius, *or* that galaxies at these distances are more clustered than their surroundings. The first hypothesis was ruled out by our study of the cross-correlation function in the previous section. We note that *both fossils and non-fossils show this increase in all redshift snapshots*, although it is more pronounced for regions around fossil groups at $z = 0$.

4.1. The behaviour of the bumps

In this section, we analyse the position and amplitude of the bump observed in the local density profile, focusing on their depedence on group properties.

4.1.1. The apparent movement

When analysing the bumps for the different evolutionary stages, it can be seen that they become more pronounced towards z=0, but that they also seem to be moving closer to the group. Our analysis shows that most of the galaxies located at the position of the bump at a given redshift, are also positioned in the region of the bumps in later outputs. This finding leads us to rule out the possibility of rebound galaxies (Mamon et al. 2004; Gill et al. 2005; Mamon 2006) being the cause of the bump since these galaxies are expected to dramatically change their positions with respect to the group centre between redshifts 0.69 and 0.00. The apparent movement of the bump could therefore be the result of either infalling substructure *or* simply the growth of the virial

---

[2] We refer to the region where the local density increases outside the virial radius as the "bump".

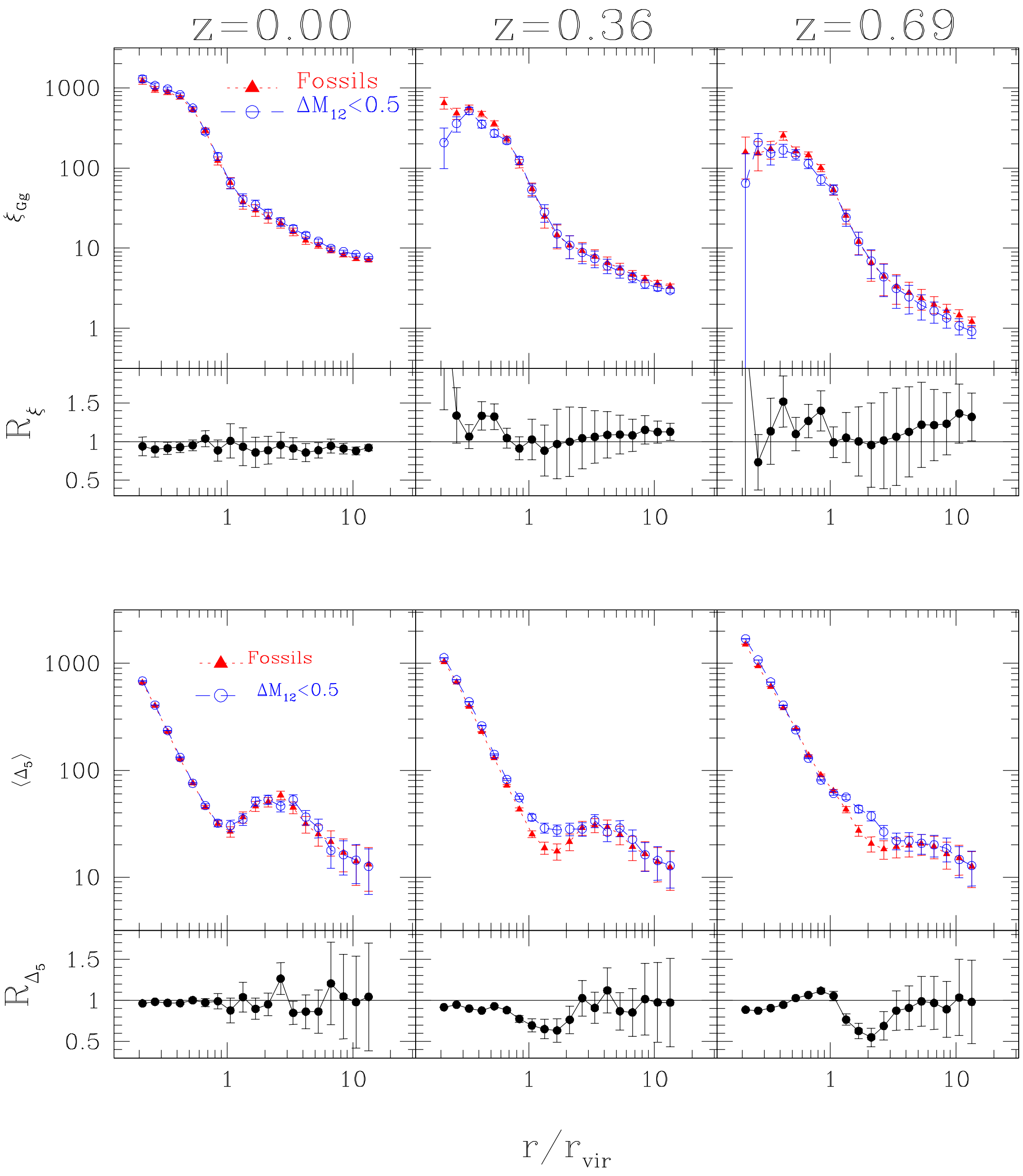

Fig. 5. Same as Fig. 2 but for the sub-samples of fossils and non-fossils with the same virial mass and assembly time distributions (samples in right panels of Fig.1).

radii of the systems concerned, i.e. the physical location of the bump being fixed. The *upper panel* of Fig. 3 shows the variation in the virial radius with time. It can be seen that the median of the virial radius for fossils increases from ∼1.1 $Mpc\ h^{-1}$ at $z = 0.69$ to ∼1.7 $Mpc\ h^{-1}$at $z = 0.00$. The bump in the local density profile for fossil groups at z=0.69 is positioned at $r/r_{vir} \sim 4.5$, which in physical units corresponds to $\sim 5\ h^{-1}Mpc$. If the galaxies in the bump possess no significant proper motions with respect to the cluster centre, then we should find the bump at 2.9 r_{vir} at redshift z=0.00, i.e., we should see an *apparent* movement simply because the size of the groups increases with time. However, it can be seen that the position of the bump at z=0.00 is ∼ 2.5 r_{vir}, which indicates that besides the apparent movement caused by the change in size, there is also a real movement of the particles in the bump towards the centre of the group. The proper motions of galaxies in the bumps have to account for a movement of less than $0.5r_{vir}$, which means that those galaxies have to have radial velocities with respect to the centre of the groups of $0.5r_{vir}/\Delta t \sim 850h^{-1}kpc/6.118Gyr = 1164kpc/6.118Gyr \sim 185\ km/s$.

4.1.2. Dependence on the assembly times

It is well known that both the mass and assembly times of the systems are affected by their environment (Espino-Briones et al. 2007). It is widely accepted that fossil systems assembled earlier than non-fossils (D'Onghia et al. 2005; Dariush et al. 2007; Díaz-Giménez et al. 2008). Hence, the following question arises: how does the assembly time of the systems affect the local density profiles? To answer this question, we re-sampled the mass-matched samples according to their assembly times[3]. We also restricted the samples to $\mathcal{M}_{\rm vir} < 10^{14} h^{-1} \mathcal{M}_\odot$ to avoid differences being caused by any differences in mass. Figure 4 shows the local density profiles for systems with early assembly times (> 80th percentile of the distribution of assembly times)(*dotted lines*), and systems that assembled later (< 20th percentile of z_a) (*dashed lines*).

---

[3] According to the definition of De Lucia et al. (2006), we take the assembly time z_a to be the time when the system has acquired 50% of its final ($z = 0.0$) virial mass.

The effect of the assembly time on the local density profile is clear: *Systems that assembled earlier show a more pronounced bump than systems that assembled later*, and this is true for both fossils *and* non-fossils.

It can also be seen that the local density profiles of non-fossil systems that assembled later ($z_a < 0.41$) show an inner peak, very close to the virial radius for the snapshots z=0.36 and z=0.69 (*middle and right lower panels*), and this feature can also be seen in the local density profile at z=0.69 for fossil groups with late assembly times ($z_a < 0.83$) (*right upper panel*). The snapshots at z=0.36 and 0.69 represent stages where the groups with late assembly time are not yet fully assembled (in the sense that they have not reached half of their final mass) and are therefore less relaxed. On the other hand, groups (fossils or non-fossils) with early assembly times do not show any inner peak immediately outside the virial radius. Their earlier assembly makes these groups more relaxed in the snapshots shown in Fig. 4. Therefore, the shape of the over-density profile is then influenced by the assembly time of the groups, and also by the stage of relaxation of the groups in any given snapshot.

5. Differences between fossils and non-fossils

We have demonstrated above that the local density profiles of fully assembled galaxy systems increase beyond the virial radius. We have found that galaxies remain in this region for a long time, gradually approaching the group centres. We have also shown that the shape of the local density profile and the amplitude of the bumps strongly depend on both the assembly times of the groups and their relaxation stage. This last finding might lead us to conclude that the environmental differences observed between fossil and non-fossil systems are purely an evolutionary effect since fossil groups assembled earlier. However, although fossil groups are indeed, on average, older than non-fossils, there exist sub-samples of fossils and non-fossils that assembled at similar times (see *lower left panel* of Fig. 1). Since fossils have developed the two-magnitude gap, while non-fossils do not, we are led to ask: Could the environment be responsible for this magnitude gap in fossils?

In this section, we therefore investigate whether the environment is different for fossil and non-fossils systems that have the same assembly times, and consequently, the same relaxation in any given snapshot. To this end, we select new sub-samples of fossils and non-fossils having the same z=0 virial mass *and* assembly time distributions (the assembly-matched samples; *upper right* and *lower right* panels of Fig. 1). Both of the new samples comprise ∼ 330 groups each.

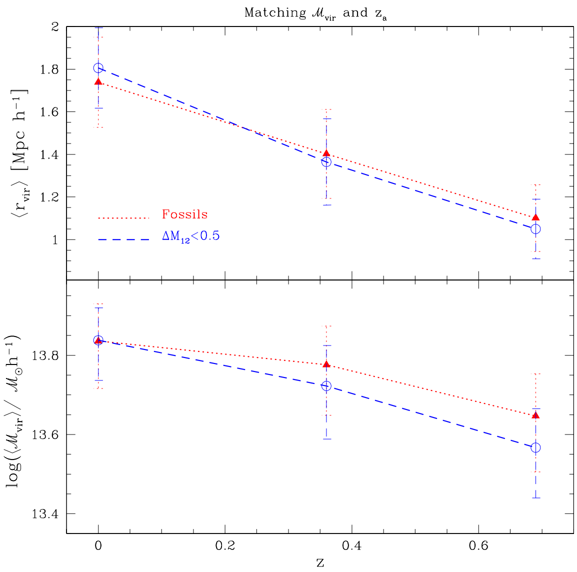

Fig. 6. Median values of virial radii (*upper panel*) and masses (*lower panel*) as a function of redshift for fossils (*dotted line*) and $\Delta M_{12} < 0.5 mag$ groups (*dashed line*) with the same mass and assembly time distributions. Error bars are the 25th and 75th percentiles.

We first calculate the cross-correlation function in order to check whether the differences observed in the *upper panels* of Fig. 2 persist. The upper panels of Fig. 5 show the cross-correlation function for these new samples. Comparing these figures, the strong differences seen, particularly at the earliest snapshot (z=0.69), have become smaller. However, the tendency of fossil groups to be in higher number density regions at high z is still present, although it is clearly somewhat weaker. To confirm this trend, we analysed the evolution of the halo virial masses for the assembly-matched samples. In the *lower panel* of Fig. 6, the medians of the halo masses at the different snapshots are shown. As can be seen, at z=0, the fossil and non-fossil halos have the same mass (by construction). However, at higher z, fossils exhibit higher halo masses. This is an interesting result since both samples have the same final mass and assembled at the same time. The result supports the weak trend observed at high z in the cross-correlation function. A higher number density around fossils clearly allows these groups to reach higher masses than non-fossils in the same period of time. Hence, the environment of fossils and non fossils are different even for the assembly-matched samples, indicating that the differences are a matter not only of time evolution.

We next calculate the local density profiles for the assembly-matched samples. The *bottom panels* of Fig. 5 show the local over-density profiles for these new samples. Comparing these results with those found in Sect. 4, it can be seen that the local over-density inner peak observed just outside the virial radius of non-fossils at z=0.36 and 0.69 is drastically reduced, as a result of our having discarded the least relaxed non-fossil systems. Moreover, at z=0, the bumps for fossils and non-fossils became similar, which indicates that the difference observed for the mass-matched samples at this snapshot is due only to differences in the assembly times of the groups involved. However, *the main differences between fossils and non-fossils observed at earlier evolutionary stages are still present despite there no longer being any assembly time dependence*. This is a very interesting result as it indicates that the environments of fossils and non-fossils are indeed intrinsically different at high redshift, and may therefore be the cause of the differences in the magnitude gaps among these systems.

6. Comparison with observations

The most interesting result we have found is related to the local over-density profile at redshift zero. From this profile, we observe that the environments of *simulated* fossil systems look

Table 1. Observational Fossil and Normal Groups

Fossil Groups	z	σ_v $[km\ s^{-1}]$	$r_{\rm vir}$ $[h^{-1}\ Mpc]$	L_X $[erg\ s^{-1}\ 10^{43}]$
RXJ1340+4018	0.171	706	1.05	1.24
RXJ1159+5531	0.081	435	1.08	1.14
RXJ1416+2315	0.138	500	1.49	6.09
RXJ1552+2013	0.136	459	1.22	2.29
Normal Groups				
400d-177	0.169	680	1.22	2.55
400d-081	0.064	449	1.25	2.24
400d-151	0.160	502	1.06	1.26
400d-180	0.167	452	1.33	3.88

Notes: Normal groups were extracted from the 400d Cluster Catalogue http://hea-www.harvard.edu/400d/catalog/table_cat.html

different from the environments of normal groups. Is it possible to observe the same behaviour of the local over-density for a sample of observational fossil systems?

To answer this question, we selected small samples of fossil and normal systems from a large-scale galaxy survey. We used the main spectroscopic sample of galaxies of Sloan Digital Sky Survey Data Release 7 (SDSS DR7, Abazajian et al. (2009)) and, following the work of Voevodkin et al. (2009), selected four known fossil groups from their sample. We also constructed a sample of four normal groups from the 400d Cluster Catalogue (Burenin et al. 2007). The normal groups were selected to ensure that the groups had similar radial velocity dispersions and mean redshifts to those in the fossil sample. The velocity dispersion restriction was imposed in order to match the virial mass distribution criterion adopted in the simulations, while the redshift restriction was designed to reduce the number density dependence on distance. The virial radii of the systems were computed from their X-ray luminosity following Vikhlinin et al. (2009) and Voevodkin et al. (2009). Details of the systems are given in Table 1.

In the work presented above, we have defined the local over-density in the simulation using the full three-dimensional (3D) spatial information. This is obviously not possible with observational data. In addition, the observable samples of galaxies are apparent-magnitude-limited, and the computed local densities will therefore depend on the redshifts of the groups. Consequently, we slightly modified the way of measuring local over-densities in the observational data. Our procedure is as follows:

1. We select a spectroscopic sample of galaxies around each group consisting of galaxies within 1000 km/s of the group centre to avoid projection effects.
2. We then select galaxies brighter than the absolute magnitude limit that corresponds to the farthest redshift allowed ($v_{max} = v_r + 1000\ km/s$) (volume limited sample).
3. We measure *projected* local densities using the third closest neighbour (Σ_3).
4. We compute the mean projected local density corresponding to the redshift of the group $\Sigma_3(z)$.
5. We compute the projected local over-density as $\Delta_3 = \frac{\Sigma_3 - \bar{\Sigma}_3(z)}{\Sigma_3(z)}$.
6. We compute the projected local over-density profile as a function of the normalised *projected* distance to the centre.

The projected local over-density profiles in the observational data are shown in the left panel of Fig. 7. This figure shows that the bump observed beyond the virial radius in the simulated fossil groups is also present in the observational sample. However, it can also be seen that the ratio of the local over-density profiles (R_{Δ_5}) *within* 1 r_{vir} of systems in the observations differs from that shown in Fig. 2 (lower left panel), with galaxies in fossil systems exhibiting significantly lower relative local over-densities than their counterparts in normal systems. However, this can be understood in terms of the differing luminosity limits applied to the two analyses, i.e., since we consider fossils, we expect, by definition, to find a lack of bright galaxies in the proximity of the central galaxy compared to similar regions in the normal systems, while faint galaxies should be equally distributed in both samples. This is only discernible when working on observational samples that are magnitude limited, since only the brightest galaxies are observed.

To perform a fair comparison between observations and semi-analytic models, it is particularly helpful to construct a mock galaxy catalogue. We therefore used the semi-analytical model to build a mock sample of galaxies within a cone consisting of shells constructed from different snapshots corresponding to the epoch of the look-back time at their distance. Here we use the 17 last snapshots, bringing us to a maximum redshift of $z = 0.68$. For the mock galaxies, we obtain redshifts by adding the Hubble flow to the peculiar velocities projected along the line-of-sight direction. We compute the observer-frame galaxy apparent magnitudes from the rest-frame absolute magnitudes provided by the semi-analytical model. These apparent magnitudes are converted to the observer frame using tabulated $k + e$ corrections (Poggianti 1997). We set an apparent magnitude limit $R = 17.44$, which roughly corresponds to the r-sdss band magnitude limit of $r = 17.77$ (see Appendix A in Díaz-Giménez & Mamon (2010)). We identify groups of galaxies in the mock catalogue following a similar procedure as Zandivarez et al. (2006). We also measure virial masses, virial radius, and radial velocity dispersions for the groups following the cited work.

Fossil and non-fossil groups are selected according to the criteria described in Sect. 2. We found ten fossil groups in the mock catalogue with a median redshift of 0.064 ± 0.015 and median group radial velocity dispersion of $338 \pm 78\ km\ s^{-1}$. We selected ten non-fossil groups among the 219 identified in the mock catalogue to reproduce the group radial velocity dispersion and redshift distributions of the fossil groups. The local over-density profile is then measured by using the same procedure described for the observational sample of groups and is shown in the *right panel* of Fig. 7. Comparing both panels, it can be seen that there is roughly an overall agreement between the profiles computed from the observations and the mock galaxy catalogue. The only noticeable difference is that the position of the bump in the observations is shifted towards larger clustercentric distances. This shifting might be, in part, a consequence of analysing slightly different evolutionary stages (z=0.13 vs. z=0.06), which would lead to the position of the bump being altered. However, this difference is also affected by the different methods employed to evaluate the virial radii (which are based on values estimated from X-ray observations for the SDSS observational sample, and the virial theorem radii in the mock catalogue).

7. Summary

We have analysed the environments around fossil and normal galaxy systems identified in the Millennium simulation (Springel et al. 2005) combined with a semi-analytical model of galaxy formation (De Lucia & Blaizot 2007). Fossil and normal systems have been selected using the same procedure as

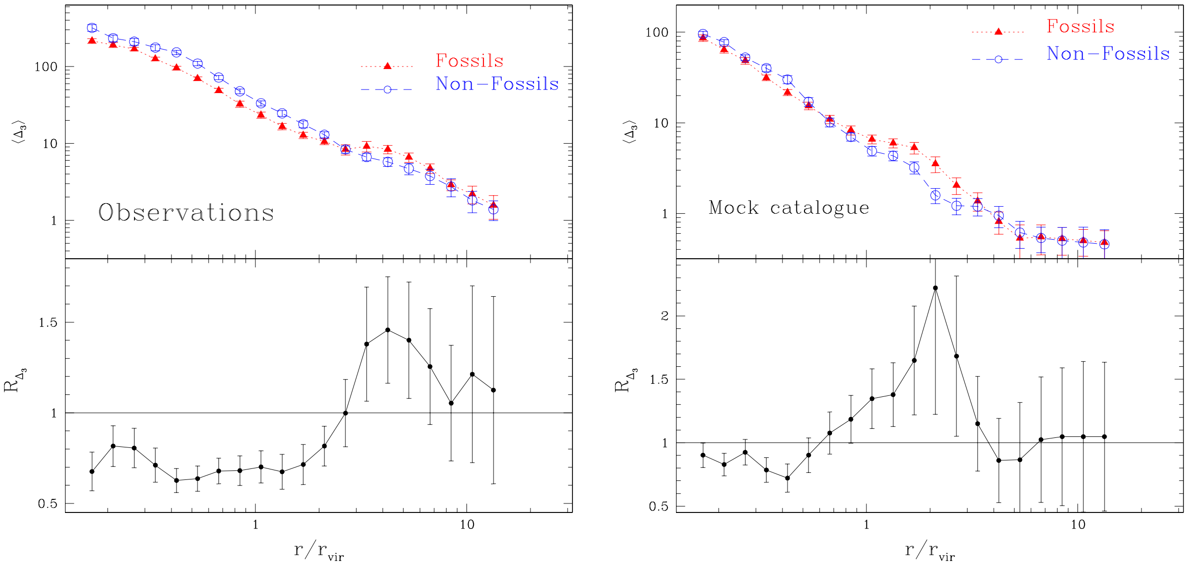

Fig. 7. Local density profile of galaxies around groups as a function of the normalised group-centric distance. Left upper panel show the local density profiles for fossils and normal systems identified observationally (see Table 1) while right upper panel show the profiles for Fossils and $\Delta M_{12} < 0.5 mag$ groups in the MS when introducing a brighter cut-off in the R-band absolute magnitude. Error bars are the 35th and the 65th percentiles in the local density distribution at each distance bin. Lower panels show the corresponding ratios of local density profiles in each case.

Díaz-Giménez et al. (2008). The samples of normal systems were divided into two sub-samples, taking into account the magnitude difference between the first and second brightest galaxies in the systems: $\Delta M_{12} < 0.5 mag$ and $0.5 mag \leq \Delta M_{12} < 2 mag$. These sub-samples were constructed to reproduce the virial mass distribution of fossils to avoid introducing a mass bias. The results obtained for these two samples of non-fossils are almost identical. We note that adopting any specific semi-analytical model introduces a dependence of the results on the particular set of parameters and physical processes that were used in the model construction. Since this work is intended to continue the analyses began by Díaz-Giménez et al. (2008), analysing the differences caused by using different semi-analytical models are beyond the scope of this work. However, we note that the model of (De Lucia & Blaizot 2007) used in this work was shown to reproduce the bright end of the luminosity function, to which our work is most sensitive, very well (Bertone et al. 2007).

We have investigated the environments using two different approaches, one global, the other local. We firstly studied the global density of galaxies as a function of the normalised group-centric distance by means of the two-point cross-correlation function. Secondly, we focused on the variation in the local density around galaxies as a function of the normalised group-centric distance by using the local density profile. From the global density analysis, we observed that at z=0.36 and earlier fossil systems in the MS were surrounded by denser regions than normal systems. This result is consistent with the common idea that galaxy systems that collapsed earlier lay preferentially in higher density regions. Following the evolution of these systems to the present day ($z = 0$), we found that the outskirts of galaxy systems in the MS have evolved differentially, finally, at $z = 0$, reaching a point where the regions surrounding fossils are slightly *under-dense* compared to normal systems. This last result agrees with some observational results that studied fossil groups at low redshifts (Adami et al. 2007).

From the local density point of view, the local density profiles have yielded very interesting results. We measured an increase in the local density profiles in the outskirts of groups for both fossil and non-fossil samples at $z = 0$, but fossils clearly exhibit a sharper increase. This local density bump is observed for fossil systems in every redshift snapshot, decreasing their amplitude and shifting toward higher distances as we move backwards in time. The difference in the local density profiles at $z = 0$ between fossils and non-fossils occurs at $\sim 2.5\, r/r_{vir}$, and indicates a clear difference exists between the environmental distributions.

Even though fossil systems have relatively under-dense regions in their outskirts according to the global density results, the local density analysis implies that galaxy clumps are more concentrated around fossils than around normal systems at z=0.

To address these differences in the environments, we have performed several tests:

- Firstly, in the local density profile, we have found that the apparent movement of the bump with time is not due entirely to the growth of the groups with time, but also to the motion of the galaxies in the over-densities towards the centres of the groups.
- Secondly, we divided the samples of both fossil and normal systems into two disjoint sub-samples according to their assembly times (corresponding to a *early* and *late assembly*). The local density profiles demonstrate that, for both samples, the earlier the groups assembled, the larger the amplitude in the local density bump is. Hence, we have demonstrated that the formation time of groups is reflected in the amplitude of this local density feature. This result is quite interesting since the local density profile emerges as a new statistical tool suitable for distinguishing the formation epoch of galaxy systems at $z = 0$, and also defining the virialised region of systems.
- Thirdly, to avoid the assembly-time influence on the environment, we have constructed new sub-samples of fossil and

non-fossil groups with similar virial mass and assembly time distributions. The cross-correlation function and the local density profiles for these new sub-samples have shown that, even when the groups have formed at similar times, the environments around fossils differ intrinsically from those observed surrounding non-fossil groups at earlier evolutionary times. Therefore, this result suggests that environment does play an important role in the fossil formation scenario.

Porter et al. (2008) studied structures around clusters, and found an increment in the star formation activity, peaking at approximately twice the virial radius of the clusters. They hypothesised that an increase in the local density of galaxies at about twice the virial radius could explain the increased galaxy star formation in terms of galaxy-galaxy harassment. This theory is strongly supported by the results found in our work here because we have been able to effectively measure the increase in the local density that could lead to efficient galaxy interactions.

Our results also encouraged us to investigate whether these features in the local density profile are measurable for observational fossil systems. We have computed the projected local density profile for four well-known fossil groups and four normal groups, both samples having similar physical properties. Our results suggest that, even with poor statistics, we can obtain similar results to those obtained from the numerical simulations. We have found a clear increase in the local density profile for the fossil sample.

Acknowledgements. We thank the anonymous referee for helpful comments and suggestions. The Millennium Simulation databases used in this paper and the web application providing on-line access to them were constructed as part of the activities of the German Astrophysical Virtual Observatory. This work was partially supported by the Consejo de Investigaciones Científicas y Técnicas de la República Argentina (CONICET) and Secretaría de Ciencia y Técnica, UNC (SeCyT). CMdO acknowledges financial help from FAPESP through the thematic project 01/07342-7. L.R.A. would like to thank FAPESP, CNPq and the Pró-Reitoria de Pesquisa, Universidade de São Paulo, for support.

References

Abazajian, K. N., Adelman-McCarthy, J. K., Agüeros, M. A., et al. 2009, ApJS, 182, 543
Adami, C., Russeil, D., & Durret, F. 2007, A&A, 467, 459
Berlind, A. A., Kazin, E., Blanton, M. R., et al. 2006, ArXiv Astrophysics e-prints, 0610524
Bertone, S., De Lucia, G., & Thomas, P. 2007, MNRAS, 379, 1143
Burenin, R. A., Vikhlinin, A., Hornstrup, A., et al. 2007, ApJS, 172, 561
Cypriano, E. S., Mendes de Oliveira, C., & Sodr, L. J. 2006, AJ, 132, 514
Dariush, A., Khosroshahi, H., Ponman, T., et al. 2007, MNRAS, 382, 433
Dariush, A. A., Raychaudhury, S., Ponman, T. J., et al. 2010, MNRAS, 405, 1873
De Lucia, G. & Blaizot, J. 2007, MNRAS, 375, 2
De Lucia, G., Springel, V., White, S., Croton, D., & Kauffmann, G. 2006, MNRAS, 366, 499
Díaz-Giménez, E. & Mamon, G. A. 2010, MNRAS, 409, 1227
Díaz-Giménez, E., Muriel, H., & Mendes de Oliveira, C. 2008, A&A, 490, 965
D'Onghia, E., Sommer-Larsen, J., Romeo, A., et al. 2005, ApJ, 630, L109
Espino-Briones, N., Plionis, M., & Ragone-Figueroa, C. 2007, ApJ, 666, L5
Gao, L., Springel, V., & White, S. D. M. 2005, MNRAS, 363, L66
Gill, S. P. D., Knebe, A., & Gibson, B. K. 2005, MNRAS, 356, 1327
Harker, G., Cole, S., Helly, J., Frenk, C., & Jenkins, A. 2006, MNRAS, 367, 1039
Jing, Y. P., Suto, Y., & Mo, H. J. 2007, ApJ, 657, 664
Jones, L. R., Ponman, T. J., Horton, A., et al. 2003, MNRAS, 343, 627
Khosroshahi, H. G., Ponman, T. J., & Jones, L. R. 2006, MNRAS, 372, L68
Mamon, G. A. 2006, in Groups of Galaxies in the Nearby Universe, ed. V. I. . J. B. I. Saviane (Berlin: Springer), 197–213, arXiv:astro-ph/0607482
Mamon, G. A., Sanchis, T., Salvador-Solé, E., & Solanes, J. M. 2004, A&A, 414, 445
Mendes de Oliveira, C., Cypriano, E., & Sodr, L. J. 2006, AJ, 131, 158
Mendes de Oliveira, C. & et al. 2008, submitted to AJ
Milosavljević, M., Miller, C. J., Furlanetto, S. R., & Cooray, A. 2006, ApJ, 637, L9
Peacock, J. A. 1999, Cosmological Physics, ed. J. A. Peacock (Cambridge, UK: Cambridge University Press, 1999)
Poggianti, B. M. 1997, A&A, 122, 399
Porter, S. C., Raychaudhury, S., Pimbblet, K. A., & Drinkwater, M. J. 2008, MNRAS, 388, 1152
Sales, L., Navarro, J., García Lambas, D., White, S., & Croton, D. 2007, MNRAS, 382, 1901
Sheth, R. K. & Tormen, G. 2004, MNRAS, 350, 1385
Springel, V., White, S. D. M., Jenkins, A., et al. 2005, Nature, 435, 629
van den Bosch, F. C., Yang, X., Mo, H. J., et al. 2007, A&A, 376, 841
Vikhlinin, A., Burenin, R. A., Ebeling, H., et al. 2009, ApJ, 692, 1033
Vikhlinin, A., McNamara, B., Hornstrup, A., et al. 1999, ApJ, 520, L1
Voevodkin, A., Borozdin, K., Heitmann, K., et al. 2009, ArXiv e-prints, 0902.0619
von Benda-Beckmann, A. M., D'Onghia, E., Gottlöber, S., et al. 2008, MNRAS, 386, 2345
Wetzel, A. R., Cohn, J. D., White, M., Holz, D. E., & Warren, M. S. 2007, ApJ, 656, 139
Yang, X., Mo, H. J., van den Bosch, F. C., et al. 2005, MNRAS, 362, 711
Zandivarez, A., Martínez, H. J., & Merchán, M. E. 2006, ApJ, 650, 137
Zandivarez, A., Merchán, M. E., & Padilla, N. D. 2003, MNRAS, 344, 247